The Kauai Experiment

Michael B. Porter, Paul Hursky, Martin Siderius[1], Mohsen Badiey[2], Jerald Caruthers[3], William S. Hodgkiss, Kaustubha Raghukumar[4], Daniel Rouseff, Warren Fox[5], Christian de Moustier, Brian Calder, Barbara J. Kraft[6], Keyko McDonald[7], Peter Stein, James K. Lewis, and Subramaniam Rajan[8]

[1]*Center for Ocean Research, SAIC, San Diego, CA*
[2]*University of Delaware, Newark, DE*
[3]*University of Southern Mississippi, Stennis Space Center, MS*
[4]*Marine Physical Laboratory, Scripps Institution of Oceanography, La Jolla, CA*
[5]*Applied Physics Laboratory, University of Washington, Seattle, WA*
[6]*Center for Coastal and Ocean Mapping, University of New Hampshire, Durham, NH*
[7]*Space and Naval Warfare Center, San Diego, CA*
[8]*Scientific Solutions, Inc., Nashua, NH*

Abstract. The Kauai Experiment was conducted from June 24 to July 9, 2003 to provide a comprehensive study of acoustic propagation in the 8-50 kHz band for diverse applications. Particular sub-projects were incorporated in the overall experiment 1) to study the basic propagation physics of forward-scattered high-frequency (HF) signals including time/angle variability, 2) to relate environmental conditions to underwater acoustic modem performance including a variety of modulation schemes such as MFSK, DSSS, QAM, passive-phase conjugation, 3) to demonstrate HF acoustic tomography using Pacific Missile Range Facility assets and show the value of assimilating tomographic data in an ocean circulation model, and 4) to examine the possibility of improving multibeam accuracy using tomographic data. To achieve these goals, extensive environmental and acoustic measurements were made yielding over 2 terabytes of data showing both the short scale (seconds) and long scale (diurnal) variations. Interestingly, the area turned out to be extremely active with a large mixed layer overlying a very dynamic lower channel. This talk will present an overview of the experiment and preliminary results.

OVERVIEW

The site of the experiment at the Pacific Missile Range Facility was selected primarily to take advantage of a network of over 200 hydrophones distributed over an offshore area larger than the state of New Mexico. As discussed later, this hydrophone array provides a unique capability for HF acoustic tomography. With that decided, the various participants agreed on a 6 km track following the 100-m isobath as shown in Fig. 1. Experience in other tests has shown that this length of track in this water depth typically provides an interesting combination of propagation conditions, including simple 2-path propagation in the near field and transitioning to order 10 echoes downrange (depending on bottom reflectivity). Similarly, communications work in the 8-16 kHz band has typically shown that standard sources (about 185 dB) start to fade out at the extreme of this range.

The University of New Hampshire, Center for Coastal and Ocean Mapping conducted the first stage consisting of mapping an area of approximately 100 km^2 in water depths of 30-900 m northwest of Kauai (Fig. 1). This was done with a combination of multibeam echo-sounders both capable of 150 deg swath widths: a RESON SEABAT 8111 sonar system operating at 100 kHz and used for water depths from 30 m to 400 m, and a Kongsberg EM120 sonar system operating at 12 kHz for depths greater than 400 m.

The deepwater system was permanently mounted on the hull of the ship. The shallow water sonar was installed temporarily for the purpose of this experiment, and it was deployed about 1 m deeper than the ships draft (about 5 m), which is also the baseline of the deepwater sonar, and the depth at which sound speed variations can have the most impact on beam pointing accuracy. Both sonar systems shared the same shipboard attitude and navigation sensing equipment.

The recorded soundings (pairs of (travel time, angle) for each beam for each ping) were processed and ray-traced into depths (z) and horizontal offsets (x, y) using sound speed vs. depth profiles derived from CTD and XBT casts taken throughout the survey area. The bathymetric grid shown in Fig. 1 was produced at a cell size of 20x20 m^2, with the WGS84 horizontal datum and the mean lower low water (observed tides) vertical datum.

There is currently only limited understanding of the role that different environmental factors, such as ocean structure, ocean variability, sea state, bottom roughness, currents, etc. play on noncoherent and coherent communications. Furthermore, the high frequencies imply wavelengths on the order of centimeters, which raises the concern that immeasurable quantities may play an important role.

To address these concerns, numerous environmental sensors such as an ADCP, waverider, CT sensors and thermistor strings were deployed in or near the propagation path as shown in Fig. 2. Besides the above described multibeam echosound survey, a sidescan survey was conducted after the experiment. To obtain a detailed picture of the ocean thermal structure, the thermistor strings were deployed in a curtain along the propagation path. In practice, it would have been difficult to produce a denser sampling; however, the spacing between strings took into consideration the typical correlation scale of internal waves. We will discuss the acoustic sensors in more detail below; however, receiving arrays were also deployed regularly along the propagation path to obtain a detailed sampling of the acoustic field.

ENVIRONMENTAL MEASUREMENTS

Sea state is one of the key drivers of HF propagation and communications performance. There are at least 3 factors at work here. First, a (hypothetical) static sea surface causes scattering with eventual losses of the steeper paths into the seabed. Second, the true sea surface is obviously dynamic, inducing coherence losses. Third, a rough sea leads to bubble injection and the resulting bubble clouds can cause strong attenuation in the 40 – 50 kHz band (depending on bubble size).
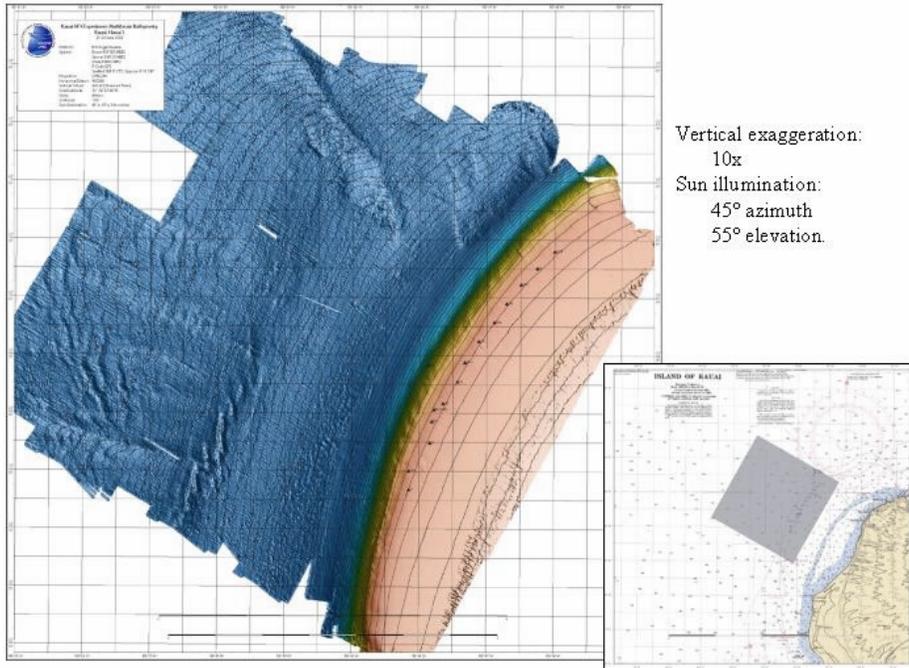
FIGURE 1. Multi-beam echo sound survey of the site and location relative to the island of Kauai (inset).
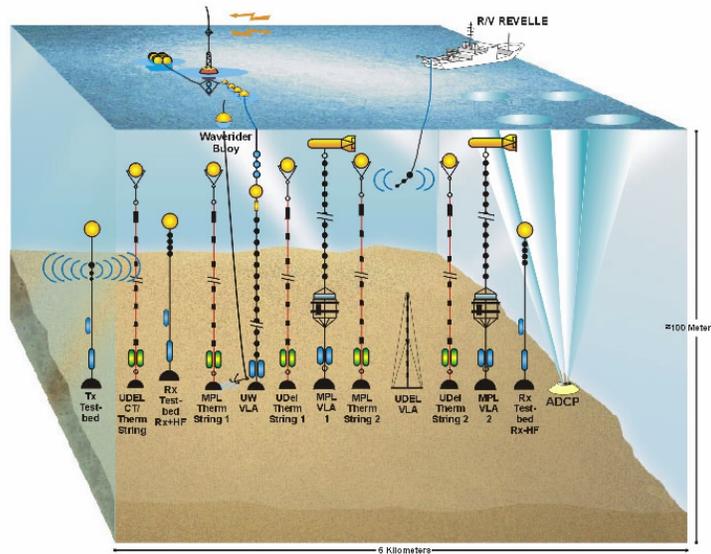

FIGURE 2. Equipment lay down for KauaiEx. The principal sound source located at the southern end (left) broadcast to VLA's distributed along the track. Acoustic sensors were interleaved with environmental sensors including thermistor strings along the entire propagation path.

The relative role of these effects is poorly understood. Indeed treatments of surface reflection are generally naïve on the role of the time scale that controls whether the surface should be treated as static or dynamic (or in between). Consider that a typical MFSK or DSSS communications system may process a 25-msec tone or symbol. This tone acoustically flashes the ocean surface capturing in a freeze frame much of the important dynamics. The treatment of these effects is an open research question; however, it was clear for the Kauai Experiment that an effort should be made to monitor the surface wave spectrum. The results in Fig. 3 show that data over the 2 weeks of the experiment.

To understand this plot it is useful to understand the surface wave behavior near Kauai. There are essentially 3 types of waves that occur: 1) long-period swell from the Southern hemisphere during the southern winter, 2) long-period swell from the northern hemisphere during the northern winter, 3) local short-period chop due to local waves. With regard to the local chop, wind on this side of Kauai follows a fairly regular pattern in which the eastern trade winds begin to pick up around noon producing a well-developed sea that then lies down in the late evening. The trade winds also have a tendency to clock around slightly to the north. The site of the experiment was purposefully selected so that the island of Kauai would cast a wind shadow on the site, which was gradually uncovered as the trade winds clocked to the north. Figure 3 shows both long and short period wave action associated with these different mechanisms.
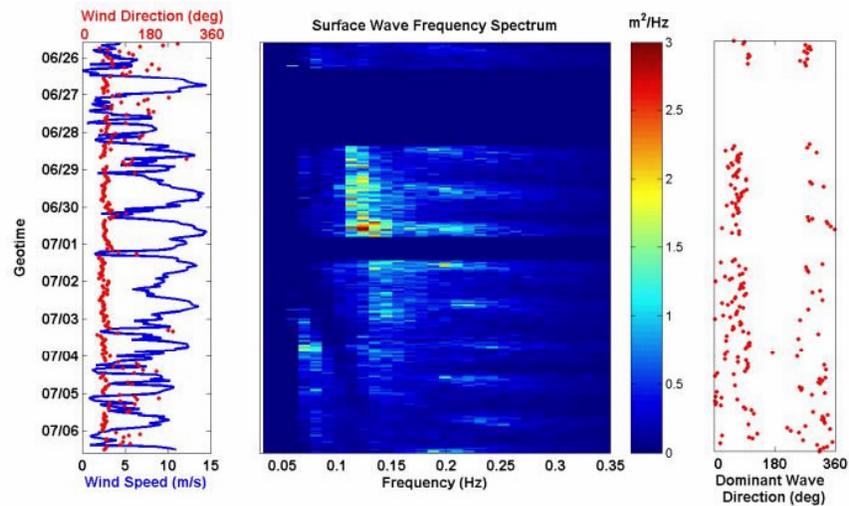

FIGURE 3. Waverider data taken over the duration of the experiment showing the daily wind cycles and associated wave spectrum.

TELESONAR TESTBEDS

The Telesonar Testbeds, developed at SPAWARSYSCEN San Diego and funded by ONR, played a central role in the experiment by providing two sound sources and two receivers. These unique, high fidelity, modular, reconfigurable, autonomous, wideband instruments were designed for high-frequency acoustic propagation and
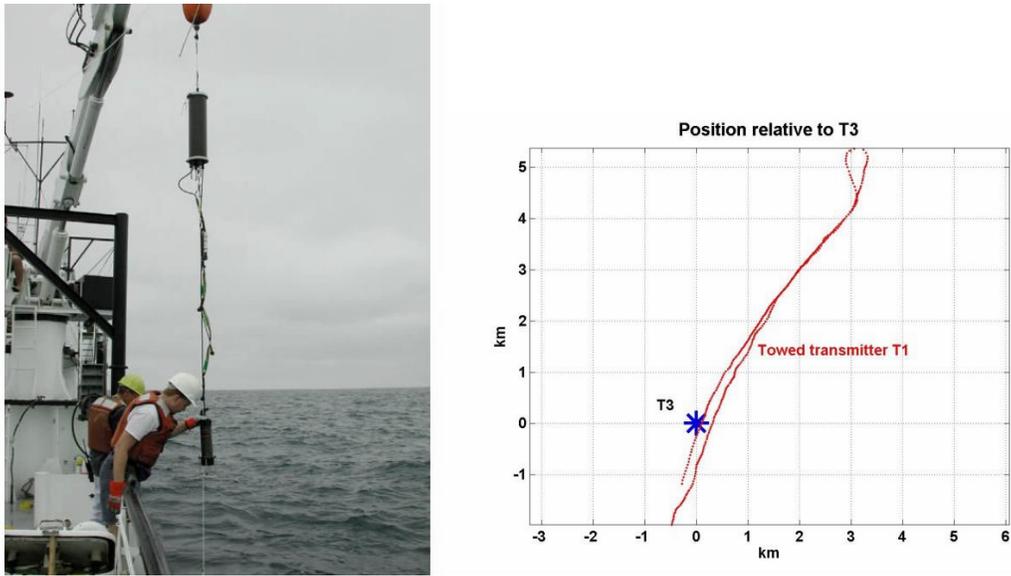
FIGURE 4. Deployment of the telesonar testbed (left). Track of the towed transmitter (T1) relative to the receiver testbed (T3) (right).
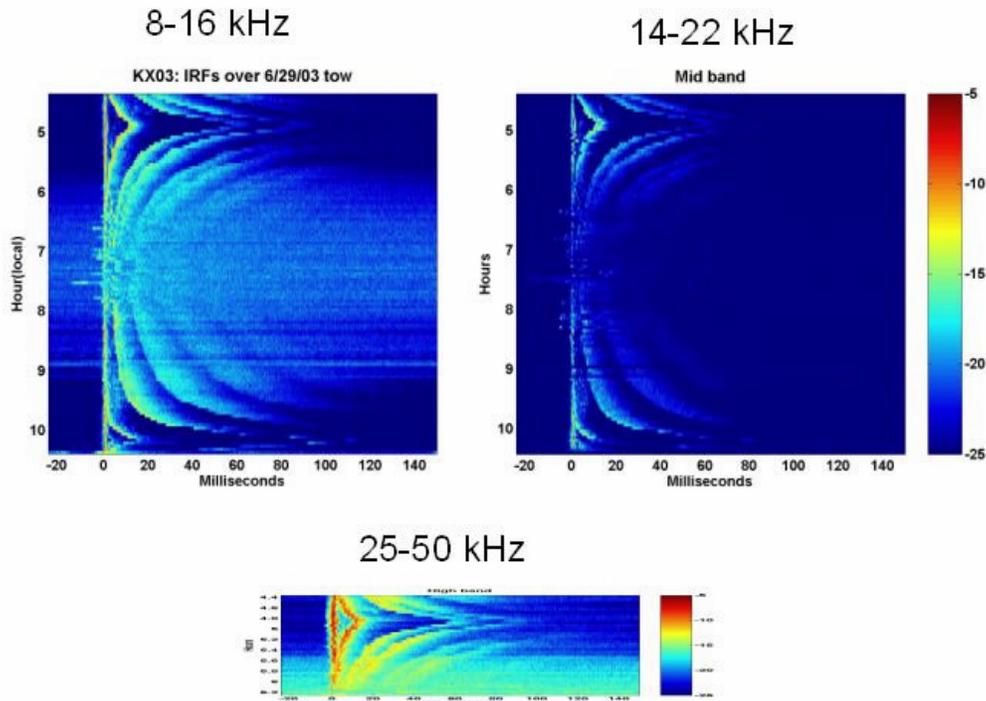

FIGURE 5. Matched-filter response or replica correlogram showing the impulse response of the channel in 3 separate frequency bands.

communication research. Each Testbed is configurable as a transmitter, receiver or both. The transmit-configured mooring is 6 meters long and has a mass of 46 kg in air 19 kg in water. This extremely small size and lightweight allow frequent field tests from an array of surface vessels down to 7 meters in length.

The Testbed transmitters are capable of sourcing arbitrary waveforms at 183 dB in three frequency bands, i.e. 8-16, 14-22, 25-50 kHz. The receiver-configured Testbeds are instrumented with a 4-channel 1.5 – 22 kHz, and a 2 channel 1.5-50 kHz receive arrays. Inside the electronics canister, a microcontroller coordinates the mission. A single-board computer running a robust real-time operating system under DOS orchestrates the sourcing and recording of data from and to a hard-disk drive. A MFSK modem is incorporated into the instrument to provide a link for remote control and status. The microcontroller, robust real-time operating system, and the modem all combine to ensure reliable mission execution. The paper by McDonald, et al. [1] provides additional information on the testbeds and their use.

Figure 4 shows the deployment of one of these systems with a PC104 computer housed in the aluminum pressure case linked to a 3-band transmitter system. The principle source unit or *diva* was deployed at the southern axis of the propagation track with the remaining VLA's providing the audience. An additional unit was towed in various patterns around the main propagation path to look at off-axis propagation and multi-user communications. Towed sources are also critical for understanding modem sensitivity to Doppler effects. As a corollary modem researchers view these measurements as either worthless or critical depending on whether they are interested in fixed or mobile networks.

An example of one such source tow is shown in Fig. 4 in which a testbed was towed to a range of about 6 km and back. Range here is measured with respect to the receiver testbed (T3) shown as the third mooring from the left in Figure 2. This sort of measurement is very useful to understand the range-dependence of the multipath structure. In addition, because the telesonar testbeds have an unusually large bandwidth, we are able to examine changes in both propagation physics and communications performance across that same large band.

Figure 5 shows the expansion and contraction of the multipath pattern as the source moves out in range then back derived by matched-filter processing. For those not familiar with the standard 'matched-filter' or 'replica correlation' procedure, we briefly review that. A chirp (also known as a linear frequency modulated sweep or LFM) is transmitted in the band of interest. The received waveform is then correlated with the transmitted waveform. Since the transmitted waveform of the chirp has a flat power spectrum, its autocorrelation produces a much shorter impulsive function (technically a sinc-pulse). The channel is considered as a linear filter so that the process of correlation can be done on the received waveform with the same effect as if it had been done to the chirp before it was transmitted. Thus, correlating the received waveform with the transmitted waveform is equivalent to transmitting an impulsive sinc function and yields an estimate of the channel impulse response.

The individual panels show the different frequency bands (low, mid, and high). We find many researchers not familiar with this frequency band are very surprised to observe a clear multipath structure involving many boundary interactions. These results clearly show this feature, even in the highest band. This multipath pattern
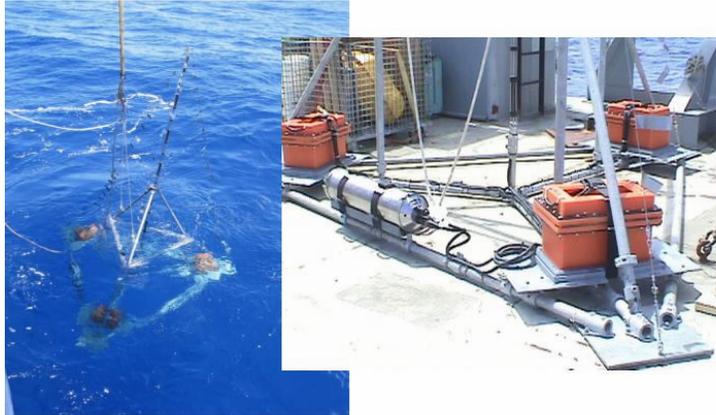
FIGURE 6. The right panel shows the Data Acquisition Unit (DAU) with three batteries mounted on the base of tripod supporting the vertical line array in center. The left panel shows the array during a deployment.
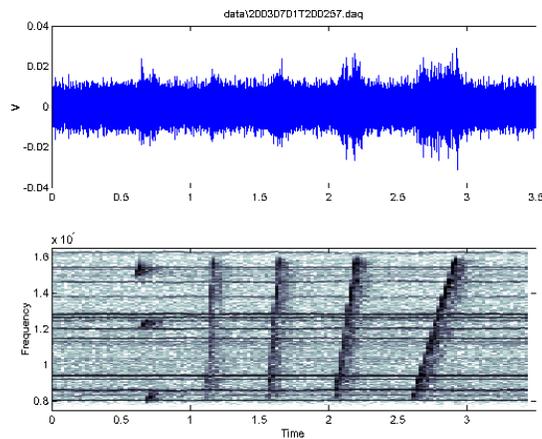

FIGURE 7. Received signal for low frequency transmissions, 8-16 kHz 320 msec. (a) Amplitude versus arrival time, (b) Frequency-time diagram for 8-16 kHz for a set of transmissions preceded by three marker tones.
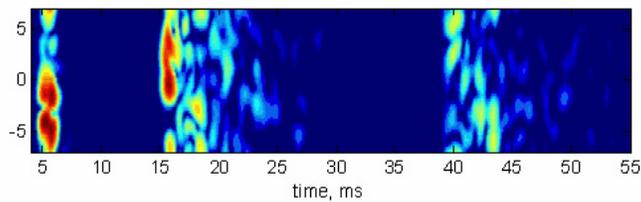

FIGURE 8. Incoming energy as a function of time and arrival angle. Note three distinct arrivals around 5-7 msec., 15-25 msec., and 40-50 msec. during 7/2/04 at 12:32 PM.

provides a unique fingerprint of the source location and can be used to track a source to many kilometers using a single phone.

MODULAR RECEIVE ARRAY

The University of Delaware designed and built a new VLA for KauaiEx using commercial off-the-shelf components. This array provided a unique capability in having enough closely spaced elements to facilitate beamforming and thereby study fluctuations in the arrival time and angle. In addition, since the array is rigid and mounted on the sea bottom, it provides a stable receiver for higher frequency signals where the effects of small array motion can influence the signal fluctuations. In this array, three batteries feed an eight channel Data Acquisition Unit (DAU) with the sampling frequency of 98 kHz. The array is lightweight and easy to deploy, requiring a winch. Figure 6 shows the VLA, the DAU and supporting tripod during one of the deployments.

To capture the effect of variability of the ocean environment on the propagation of broadband signals, a set of four LFM sweeps with variable duration were transmitted over various frequency bands every half hour. The varying durations are designed to help characterize surface variability over a very short time scale by providing different times over which to average the surface reflected signals. A single transmission consists of 9 sets of the FM sweeps 40-320 msec. in duration as shown in Figure 7. A set of three narrowband FM sweeps was used as a marker at the beginning of each transmission set; a set consists of FM sweeps over various frequency ranges. The transmissions are spaced about 3 seconds apart for a total duration of about 30 seconds.

The received signals were matched filtered and beamformed. Figure 8 shows a sample of beamformed signal depicting three distinct arrivals. The detail of the variability on the arrival energy for short and long times are shown in Ref. [2] in this volume.

AUTONOMOUS ARRAY SYSTEM

The Marine Physical Laboratory brought two water-spanning 16-channel VLA's, which provided an invaluable sampling of the acoustic field (Fig. 9). These autonomous systems are composed of a PC running Labview for data acquisition, recorded to large onboard disk drives.

Channel probes were transmitted regularly throughout the experiment to measure directly the channel impulse response. Both chirps (with pilot tones) and m-sequences were used as these each have different advantages for estimating the impulse response. An example of these receptions on the MPL array is shown in Fig. 10. Many researchers look at a single chirp and that may be said to represent a purer version of the channel impulse response. However, simply stacking the results of 20 chirps provides a vastly clearer picture of the echoes. On the other hand, if one stacks too many chirps then the temporal variations in the waveguide cause the arrivals to be smeared out. Thus, the Goldilocks solution is the figure in the middle panel.

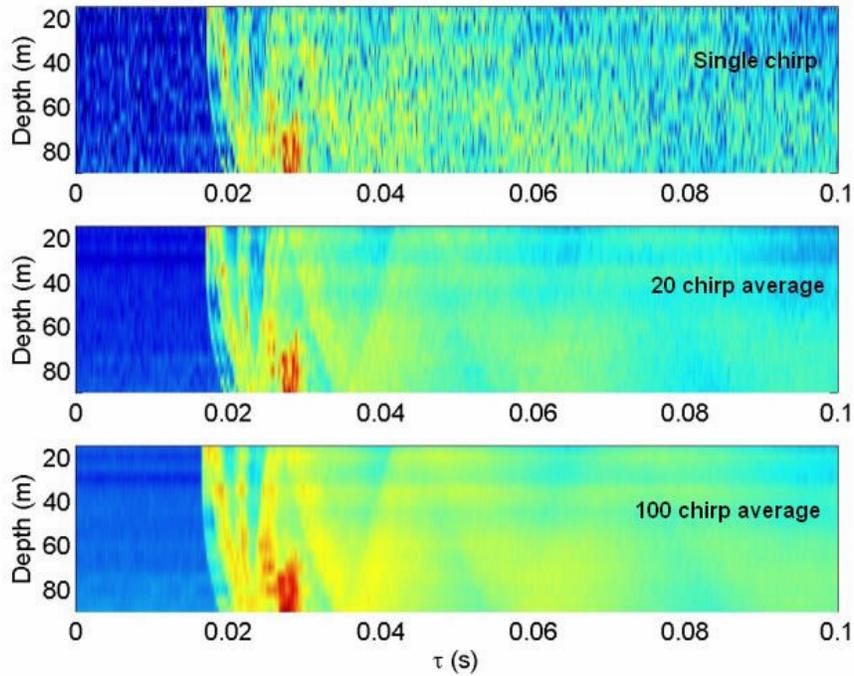**FIGURE 9.** The MPL Autonomous Array Systems laid out on deck before deployment.

FIGURE 10. Impulse response obtained by matched-filtering the data on the MPL VLA. Increasing (top to bottom) the number of chirps averaged to get the impulse response progressively draws out weaker arrivals but smears out their arrival time. Note the bottom-ducted energy showing up as a bright spot near the bottom.

In general, we may describe this as an accordion pattern where each fold in the accordion represents an additional surface or bottom reflection. The quiescent period at the beginning ends as the direct path arrives forming the first broad arc. Since the source is near the bottom, a bottom reflected path comes almost immediately behind it. There is also a significant blob of energy creeping along the bottom and arriving at about 25 msec on this time scale. These are the rays trapped in the lower sound channel that some have called the *bouncing ball* paths.

Of course, a key goal of this experiment is to understand more clearly how the propagation physics effects acoustic communications performance. Again, the MPL array provides a particularly valuable resource since it allows us to examine bit-error rates (BER) at the same time, throughout the channel.

Figure 11 shows the results from one of many schemes transmitted during the experiment. This is a multiple-frequency shift keyed system running at 2400 bps. This is arguably the simplest scheme for transmitting data and may be compared nearly precisely to the process of striking a chord on a piano. The received data is interpreted by recognizing the chords (a spectrogram) and the transmission rate is limited principally by the ocean reverberation. This in turn requires that the sound of one chord dies down before the next is played. Practical MFSK systems typically yield a bandwidth efficient of ¼ bps/Hz. Here we are using a 4800 Hz band and pushing the scheme to 2400 bps which generates somewhat high BER. However, it should be noted that in practical operation we include a half-rate convolutional coder that reduces the data rate in half but reduces the error rate to virtually zero. Since channel coding reduces the errors by a huge amount, gaining useful statistics would require many more transmissions. Therefore, we typically prefer to interpret sensitivity of the modem scheme without the channel coding.

The role of the channel on the modem performance here is obvious to the most casual observer. Large numbers of channel errors are generated in the surface mixed layer and progressively decreasing for deeper receivers. The ocean thermal structure seen in the lower panel reveals the warm mixed layer in the upper half of the water column and the cool duct at the bottom.

To discuss these effects one should be aware of numerous factors. First, the SNR is higher in the lower part of the water column, partly because of the lower duct. Ambient noise plays into that also; however, it is seen to not vary a large amount with depth. In addition, all paths in the upper mixed-layer are surface interacting causing both static and dynamic surface losses. In contrast, the bouncing ball energy in the bottom duct is strong and steady. Finally, one must consider the overall multipath spread. Increased multipath aids SNR, which is good, but causes the reverberant effect (intersymbol interference), which is bad. The paper by Siderius, et al., [3] in this volume discusses these effects in more detail.

A final point of interest in an array such as this is how multiple channels can be exploited to improve modem performance. There are many ways to think of this problem. For instance, one can imagine beamforming to a particular eigenray so that multipath spread is reduced. One can also view the receivers as being robust against fading since they fade independently (spatial diversity). A trivial way to take advantage of this spatial diversity is to process each of the channels and sum them in a sort of voting process to estimate the particular tones played. Figure 12 shows how

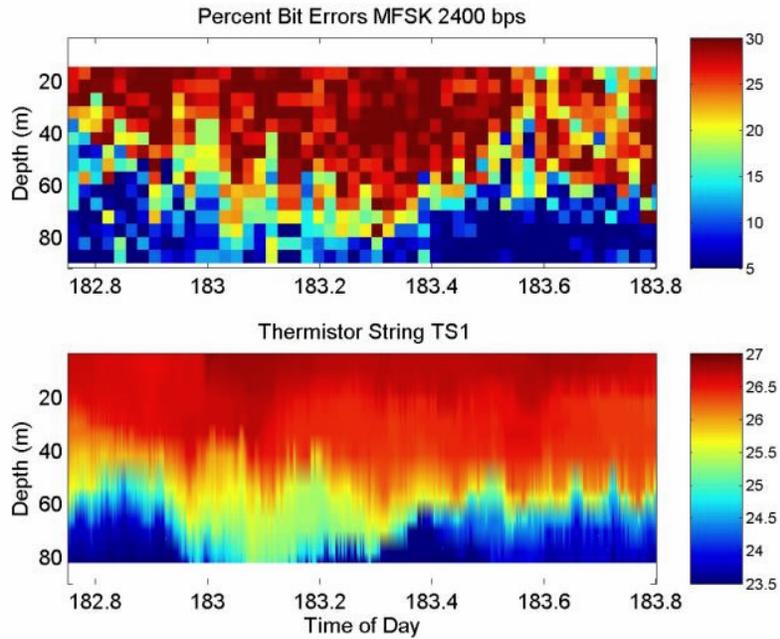summing increasing numbers of channels provides a major improvement to the system performance.

FIGURE 11. Bit-Error-Rate over depth and time (upper panel) versus the ocean temperature structure (degrees Celsius) (lower panel).
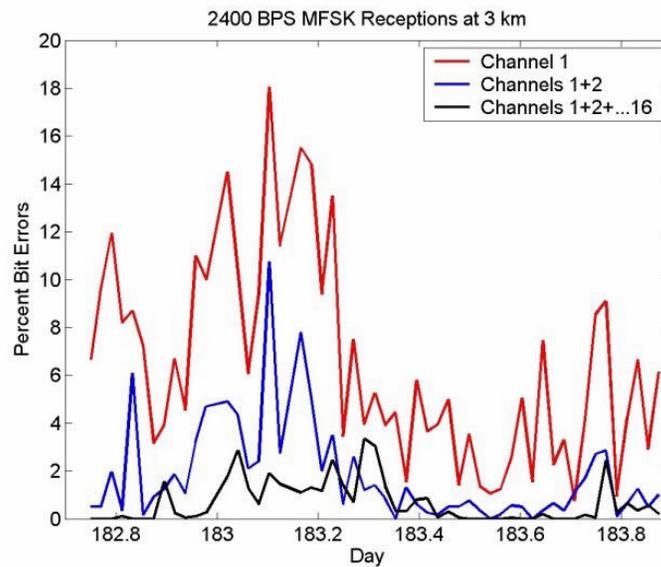

FIGURE 12. Bit-error-rates plotted vs. time and combining varying numbers of channels. Increasing the number of receivers provides a significant improvement in performance.

UW ARRAY

The UW-APL array provided another dimension to the experiment. Its 8 channels sampled a smaller slice of the water column but with greater density. In addition, the wireless access via radio buoy allowed real-time monitoring of the transmissions. The position of the array within the water column is shown in Fig. 13. One can see from the ray trace that it is poised to receive the direct and surface paths, and depending on the mixed layer depth may also get a hint of leakage energy from the bouncing ball paths.

Figure 14 shows the arrival pattern as observed down the array. Because the source is sitting on the bottom, the arrivals tend to arrive in pairs. The spacing between the array elements is 2 m and the arrival pattern shows significant structure even with this relatively dense sampling. The figure represents an average over 10 seconds so the late arriving paths that have multiple interactions with the sea surface are more diffuse than the distinct early arrivals.

HF ACOUSTIC TOMOGRAPHY

As mentioned above, a motivator for doing the experiment in this site was access to hydrophones in the Pacific Missile Range Facility. Figure 15 shows the network of sources and receivers that were used for this phase of the testing. Matched-filter output from these phones was equally successful in extracting the various boundary echoes and preliminary model runs (Figure 16) show that the arrivals for phones in deeper parts of the range are also well modeled. The paper by Lewis, et al. [4] in this volume discusses these data in greater detail.

SIDESCAN SONAR SURVEY

Finally, a sidescan survey was conducted by USM at the end of the experiment to characterize more fully the nature of the bottom. The results shown in Figure 17 are images of a small region of the bottom surveyed simultaneously with two frequencies (150 kHz on the left and 300 kHz on the right). The slant range on each side of each frequency image is 100 m and the depth, represented by the darker band down the middle of each, is 20 m. (The other dark vertical bands are nulls in the sidelobes. The wider dark band on the right side of the 300-kHz image is just incidental to the gain setting.) The speckled structures are the echoes from two fish schools (partly directly under the boat, but also off to the right side). Further to the right (offshore) and left (in shore) are sand ripples (not too clear in these figures), eventually giving way to the larger-scale ridge structures on the shoreward side also seen in the multibeam survey.

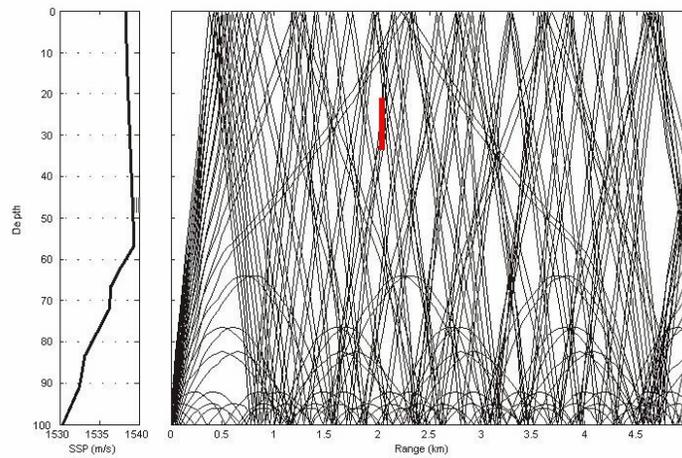The paper by Caruthers, et al. [5] presents a fuller discussion of the sidescan survey.
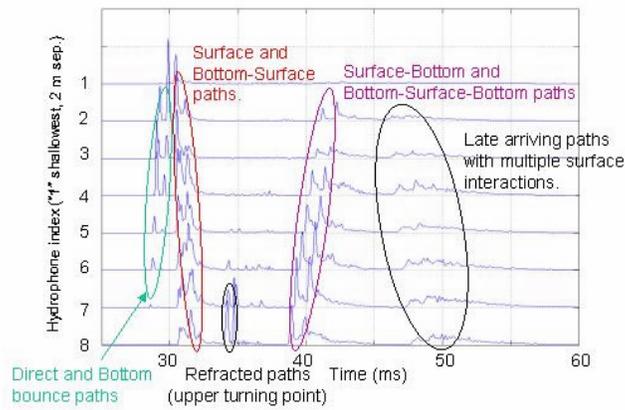
FIGURE 13. Sound-speed profile and ray trace for KauaiEx.

FIGURE 14. Matched-filter response for the UW array. Various arrivals crossing the array are clearly identified.
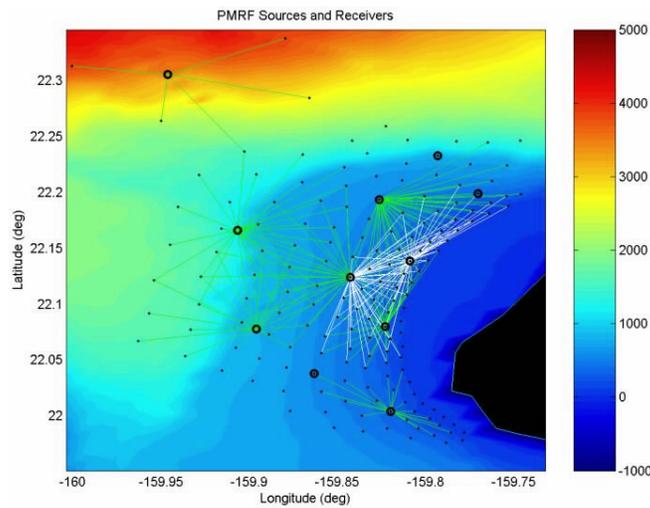

FIGURE 15. Network of sources and receivers provided by the Pacific Missile Range Facility and used for tomographic imaging of the ocean structure.
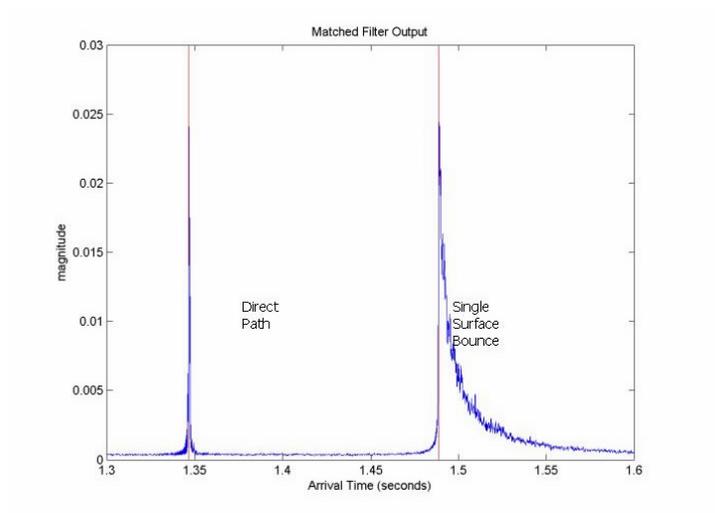
FIGURE 16. Matched-filter output from PMRF showing the two dominant arrivals in a deeper part of the range. The red curves are modeled arrival times and closely overly the blue curves derived from the data.
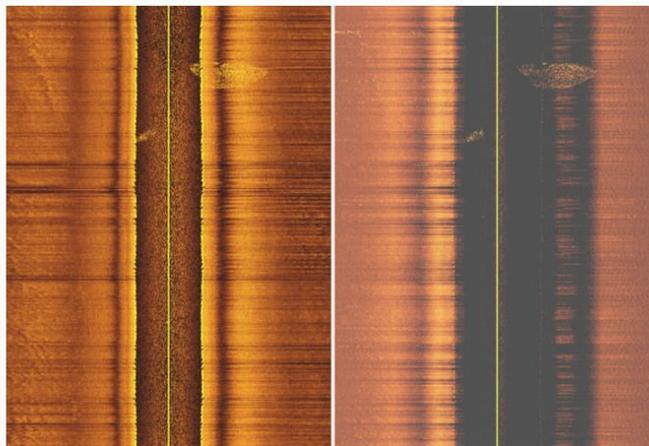

FIGURE 17. Sidescan survey images of the propagation path as seen at 150 kHz (left panel) and 300 kHz (right panel). The band down the middle represents the water depth. A school of fish is visible near the top of the plot and sand ripples along the inshore side (left).

ACKNOWLEDGMENTS

REFERENCES

1. McDonald, V., Hursky, P., and the KauaiEx Group, "Telesonar testbed instrument provides a flexible platform for acoustic propagation and communication research in the 8-50 kHz band," this volume.
2. Badiey, M., Forsythe, S., Porter, M., and the KauaiEx Group, "Effects of environmental variability on the bottom mounted vertical line array in KauaiEx," this volume.
3. Siderius, M., Porter, M., and the KauaiEx Group, "Impact of thermocline variability on underwater acoustic communications: results from KauaiEx," this volume, 2004
4. Lewis, J., Stein, P., Rajan, S., Rudzinsky, J., Vandiver, A., and the KauaiEx Group, "High-frequency tomography using bottom-mounted transducers," this volume.
5. Caruthers, J., Quiroz, E., Fisher, C., Meredith, R., Sidorovskaia, N., and the KauaiEx Group, "Side-scan sonar survey operations in support of KauaiEx," this volume.